JOURNAL OF VIROLOGY, Sept. 2005, p. 11035–11044 Vol. 79, No. 17
0022-538X/05/$08.00+0 doi:10.1128/JVI.79.17.11035–11044.2005

The Expression Strategy of Goose Parvovirus Exhibits Features of both the *Dependovirus* and *Parvovirus* Genera

Jianming Qiu,[1]* Fang Cheng,[1] Yuko Yoto,[1] Zoltán Zádori,[2] and David Pintel[1]

Department of Molecular Microbiology and Immunology, Life Sciences Center, University of Missouri—Columbia, School of Medicine, Columbia, Missouri,[1] and INRS—Institut Armand-Frappier, Université du Québec, Laval, Québec, Canada[2]

Received 20 April 2005/Accepted 3 June 2005

The RNA transcription profile of the goose parvovirus (GPV) was determined, and it is a surprising hybrid of features of the *Parvovirus* and *Dependovirus* genera of the *Parvovirinae* subfamily of the *Parvoviridae*. Similar to the *Dependovirus* adeno-associated virus type 5, RNAs transcribed from the GPV upstream P9 promoter, which encode the viral nonstructural proteins, were polyadenylated at a high efficiency at a polyadenylation site [(pA)p] located within an intron in the center of the genome. Efficient usage of (pA)p required a downstream element that overlaps with the polypyrimidine tract of the A2 3′ splice site of the central intron. An upstream element required for efficient use of (pA)p was also identified. RNAs transcribed from the P42 promoter, presumed to encode the viral capsid proteins, primarily extended through (pA)p and were polyadenylated at a site, (pA)d, located at the right end of the genome and ultimately spliced at a high efficiency. No promoter analogous to the *Dependovirus* P19 promoter was detected; however, similar to minute virus of mice and other members of the *Parvovirus* genus, a significant portion of pre-mRNAs generated from the P9 promoter were additionally spliced within the putative GPV Rep1 coding region and likely encode an additional, smaller, nonstructural protein. Also similar to members of the *Parvovirus* genus, detectable activity of the GPV P42 promoter was highly dependent on transactivation by the GPV Rep1 protein in a manner dependent on binding to a *cis*-element located in the P42 promoter.

Goose parvovirus (GPV) is the etiological agent of Derzsy's disease, also known as goose hepatitis (4, 10, 26). The single-stranded genome of GPV is 5,106 nucleotides (nt) in length and has identical U-shaped duplex terminal hairpins of 444 nt at each end (30). Both plus- and minus-strand genomes are found encapsidated into virions. The Muscovy duck parvovirus (MDPV), which was isolated from Muscovy ducks with clinical symptoms of Derzsy's disease, is highly related to GPV, exhibiting 81.9% nucleotide sequence identity (30).

Both GPV and MDPV can replicate without the aid of helper virus (9) and were originally classified in the *Parvovirus* genus, which contains other autonomously replicating parvoviruses (7). However, GPV is most closely related at the nucleotide level to adeno-associated virus type 2 (AAV2), exhibiting approximately 55% identity (1, 30), and GPV and MDPV have recently been reclassified as members of the *Dependovirus* genus (6).

In general, the protein coding organization of GPV is similar to other parvoviruses (30). The large open reading frame (ORF) in the right-hand side of the genome encodes the capsid proteins, while the large open reading frame in the left-hand side of the genome encodes the only single nonstructural protein so far identified, the 70-kDa Rep1 protein (28). GPV Rep1 and the capsid protein VP1 share, on average, approximately 62% and 70% amino acid identities, respectively, with the analogous proteins of AAV2 (although the extent of identity varies significantly within different regions of the proteins) (1, 30). Polyclonal antibody to GPV, however, does not react with AAV2 capsid proteins (16), and vice versa (J. Qiu and D. Pintel, unpublished data).

GPV Rep1 has been studied in some detail. Bacterially expressed Rep1 stimulates replication of the GPV terminal repeat in vitro and has been shown to bind strongly to a repeated GTTC element within the GPV terminal hairpin (28). Rep1 can neither stimulate replication of an AAV2 inverted terminal repeat (ITR)-containing construct nor bind efficiently to the AAV2 Rep78 Rep-binding element (RBE) (28).

In this report, we present a detailed transcription map of GPV RNA generated in goose embryonic kidney cells following transfection of an infectious GPV plasmid or following GPV infection. Surprisingly, the expression strategy of GPV was found to be a hybrid that exhibited features previously found exclusively in either the *Dependovirus* or *Parvovirus* genera of the *Parvovirinae*.

MATERIALS AND METHODS

Cells and virus. The goose embryonic kidney cell line CGBQ was obtained from the American Type Culture Collection (CCL-169). Cells were maintained in Dulbecco's modified Eagle's medium with 10% fetal calf serum at 37°C in 5% CO_2. The SMH 319 strain of GPV (ATCC VR-696) was used to infect cells at a multiplicity of infection (MOI) of 0.1.

Plasmids. (i) Construction of the full-length clone of GPV (pIGPV). GPV virion DNA (which contains both plus and minus strands) was isolated from embryonated goose eggs infected with the virulent B strain of GPV as previously described (30). Annealed viral DNA was digested with HindIII, and the two terminal fragments were cloned into the EcoRV-Hind III site of the pBluescript II SK(−) vector (Invitrogen), generating plasmids pILP12 and pILP14, respectively. The middle fragment of GPV was ligated in the HindIII site of the same vector. pILP1214 was created by digesting pILP14 with HindIII and XbaI. The XbaI site was then blunted, and the virus fragment was ligated into HindIII/SalI (blunted)-digested pILP12. The resulting plasmid contained the two complete HindIII end fragments of GPV. After HindIII digestion of pILP1214, the GPV middle HindIII fragment was inserted, generating the complete-length clone

* Corresponding author. Mailing address: 471b Life Sciences Center, 1201 E. Rollins Rd., Columbia, MO 65211-7310. Phone: (573) 882-3171. Fax: (573) 882-4287. E-mail: qiuj@missouri.edu.

pILP13 (pIGPV). The infectivity of the clone was tested by transfection into primary goose embryo fibroblasts. At 4 days posttransfection, cytopathic effect was detected in the pIGPV-transfected cells but not in mock-transfected cells (data not shown). After an additional passage, viral particles were collected by ultracentrifugation, and the pellet from pIGPV-transfected cells, but not from mock-transfected cells, contained viral particles of approximately 25 nm that were visible by electron microscopy (data not shown). A 100-μl aliquot of supernatant from the pIGPV-transfected cells, but not from mock-transfected cells, was lethal for five of five 5- to 14-day-old goose embryos at 7 days postinoculation exhibiting classic signs of parvoviral infections (data not shown).

(ii) Constructs for identification of downstream and upstream elements required for polyadenylation at (pA)p. GPVRepCap was constructed by insertion of GPV nt 314 to 4744 into pBluescript SK(+) (Invitrogen; all nucleotide numbers refer to GPV GenBank accession number U25749). To create P9JCapAA, the GPV Rep1 gene (nt 536 to 2194) in GPVRepCap was replaced with prokaryotic DNA sequences from pBR322 DNA (nt 35 to 1680), and the TAG cleavage site of the central intron A2 acceptor (nt 2454) was mutated to TAA. This mutation, which did not serve as a terminator for any known ORF, prevented splicing to either acceptor of the small intron (Qiu and Pintel, unpublished). P9JInJpAd was constructed from P9JCapAA by replacing the GPV Cap gene (nt 2456 to 4497) with DNA from λ-phage (nt 10086 to 8101). To generate plasmids P9JCapAAm6U, P9JCapAAm10U, P9JCapAAm12U, P9JCapAAm12U+GU, P9JCapAAm2U+4U, P9JCapAAm6U+2U, and P9JCapAAΔ4U+GU, the mutations diagrammed in Fig. 4, below, were introduced into P9JCapAA in the region between nt 2437 and 2472. To generate P9Im170CapAA, P9Im120CapAA, P9Im80CapAA, and P9Im40CapAA, GPV nt 2219 to 2390, 2262 to 2390, 2304 to 2390, and 2346 to 2390, in P9JCapAA, were replaced with λ DNA nt 7930 to 8101, 7978 to 8101, 8020 to 8101, and 8062 to 8101, respectively. P9mGUCapAA was constructed by mutation of the P9JCapAA GU-rich sequences at nt 2383 to ACACAAA.

(iii) Plasmids for characterization of P42 transactivation. GPVRepkoCap was made by introduction of a translation stop codon (TAA) within the *rep* gene at nt 612 in GPVRepCap. GPVΔP9RepCap was generated by deletion of sequence from nt 314 to 446 from GPVRepkoCap. Further deletion of the *rep* gene (nt 314 to 1785) from GPVRepkoCap generated the P42 minimal construct P42Cap. 2056P42Cap and 2034P42Cap plasmids were constructed by deletion of nt 1786 to 2055 and 1786 to 2033, respectively, from P42Cap. P42mRBE1Cap, P42mRBE2Cap, and P42mRBECap were constructed by mutation of the putative RBE1, RBE2, and both the RBE1 and RBE2 sites, together, in P42Cap; the exact location and type of mutation is described in the text and shown below in Fig. 6B. Addition of two synthetic RBE sequences (2× GTTCGAACGAACG AAC) (28) at nt 1786 of P42mRBECap resulted in the generation of 2×RBEP42mRBECap.

(iv) GPVRepSM. To generate GPVRepSM, silent mutations which do not change the Rep1 amino acid sequence were introduced into nt 2098 to 2120, nt 2156 to 2174, nt 2184 to 2194, and nt 2219 to 2234 of GPVRepCap. Although wild-type Rep1 protein is produced, RNAs generated from GPVRepSM by transfection are not detected by RNase protection assay (RPA) using the RP probe (see Fig. 6A, lane 2, below).

(v) Clones used to generate probes for RPA. To map the transcription unit of GPV, RPA probes, PP9, SB, RP, DH, and PpAd were constructed by cloning the following region of GPV into BamHI-HindIII-digested pGEM3Z (Promega): nt 378 to 560 (PP9), nt 881 to 1120 (SB), nt 2068 to 2263 (RP), nt 2213 to 2563 (DH), and nt 4561 to 4744 (PpAd). For the P1D and P1A probes used to map the intron in the GPV *rep* gene (intron I), GPV nt 717 to 880 and nt 1096 to 1300 were inserted into BamHI-HindIII-digested pGEM3Z (Promega). Homologous probes were constructed and used to map the downstream element (DSE) and upstream element (USE) for (pA)p; they were constructed by insertion of PCR-amplified nt 2213 to 2563 into BamHI-HindIII-digested pGEM3Z (Promega). The green fluorescent protein (GFP) probe clone was described previously (25).

All the DNA constructs were sequenced at the DNA Core of the University of Missouri—Columbia to ensure that they were as predicted.

Plasmid transient transfection. For each transfection, 2×10^6 CGBQ cells were collected and resuspended in 100 μl of solution V (Amaxa, Inc.), and 2 μg of plasmid DNA was added. Where indicated, 0.2 μg GPVRepSM and/or 0.2 μg pGFPC1 (Clontech) was cotransfected to provide Rep1 in *trans* or as an internal control. Transfection was performed by electroporation using the Amax Nucleofector device (Amaxa, Inc., Gaithersburg, Md.) using program A23. After transfection, cells were resuspended in 15 ml of Dulbecco's modified Eagle's growth medium with 10% fetal calf serum in 100-mm^2 plates. At 36 to ~40 h later, cells were harvested for RNA isolation.

RNA isolation and RPA. Total RNA was isolated using guanidine isothiocyanate and purified by the CsCl ultracentrifugation method as previously reported (27). In some circumstances, poly(A)-selected mRNA was purified by oligo(dT) magnetic beads (Dynal Biotech, Oslo, Norway). An RPA was performed as previously reported (20, 27). Probes were generated from linearized templates by in vitro transcription as previously reported (27). RNA hybridizations for RPAs were done in substantial probe excess, and RPA signals were quantified with the Molecular Imager FX and Quantity One version 4.2.2 image software (Bio-Rad, Hercules, CA). Relative molar ratios of individual species of RNAs were determined after adjusting for the number of ^{32}P-labeled uridines in each protected fragment as previously described (27). Where indicated, the signal was normalized by the internal transfection control, pGFPC1.

Northern blot analysis. Northern analyses were done as previously described (22), using either 10 μg of total RNA or mRNA isolated from 20 μg of total RNA. The ^{32}P-labeled DNA probes GPVRepCap, GPVCap, and GPVRep spanned GPV DNA sequences nt 314 to 4744, 3002 to 4744, and 314 to 1798, respectively. The DNA probes Pe1, Pi, and Pe2 contained GPV DNA sequences nt 513 to 745, 881 to 1160, and 1201 to 1920, respectively, and are diagrammed below in Fig. 2.

5′ RACE and reverse transcription-PCR (RT-PCR). Primers used for 5′ rapid amplification of cDNA ends (5′ RACE) were RGPV745 (5′-TGTTCTTGATC TTCTCTGCC-3′), RGPV1280 (5′-GTTCTCAGTGAGCCATTG-3′), and the anchored primer oligo(dT)19V (V = G or A or C). The location of these primers is shown below in Fig. 2. 5′ RACE was performed as previously described (14).

RT-PCR was performed using the Titan-One RT-PCR kit (Roche) with primers F513 (5′GAGAACGGACCTCAGGTCGG3′) and R2194 (5′TGCTTCTCT TAGGCTCAG3′), which are diagrammed below in Fig. 2. PCR DNA fragments were purified, and sequence determination was performed at the University of Missouri—Columbia DNA Core facility.

RESULTS

GPV utilizes a polyadenylation site in the center of its genome and lacks a P19 promoter that is efficiently used in CGBQ cells. The transcription map of GPV was determined following transfection of a GPV infectious clone, or following infection of GPV, into the goose embryonic fibroblast cell line CGBQ, which has previously been shown to be permissive for GPV infection (1).

Northern analysis revealed that following transfection, the full-length GPV clone pIGPV exhibited a pattern of expression similar to that previously seen for RNA generated by AAV5 (24). A probe that spanned the entire GPV Rep-Cap region detected a predominant band of 2.3 kb and three additional less-abundant bands, one larger and two smaller (Fig. 1B, lane 2). The 2.3-kb band was also detected by a probe specific for the capsid region, suggesting that it was the major capsid gene RNA (Fig. 1B, lane 4). A probe specific to the Rep1 gene did not detect the 2.3-kb species, but rather detected RNA bands of approximately 1.9 kb and 1.6 kb (Fig. 1B, lane 6). The size of these RNAs suggested that, as is the case with AAV5, the putative Rep-encoding RNAs did not extend through the polyadenylation site in the middle of the genome. Although this analysis showed similarity to the pattern of expression of AAV5 (24), as described more fully below, the origin of the 1.6-kb band was unexpected. The faint band between 3.6 kb and 4.2 kb seen in all of these blots likely represents a low-abundance RNA which extends from the Rep region through to the distal polyadenylation site.

To confirm the expression profile deduced from Northern blot analysis and to map the important landmarks of GPV RNA more precisely, we subjected GPV-generated RNA to RNase protection assays using five probes (PP9, SB, RP, DH, and PpAd) suggested by previous analysis of AAV5 (24).

The predominant band (on a molar basis) protected by the PP9 probe, which spanned the putative P9 promoter, was approximately 70 nt (Fig. 1C, lane 2). This is consistent with an

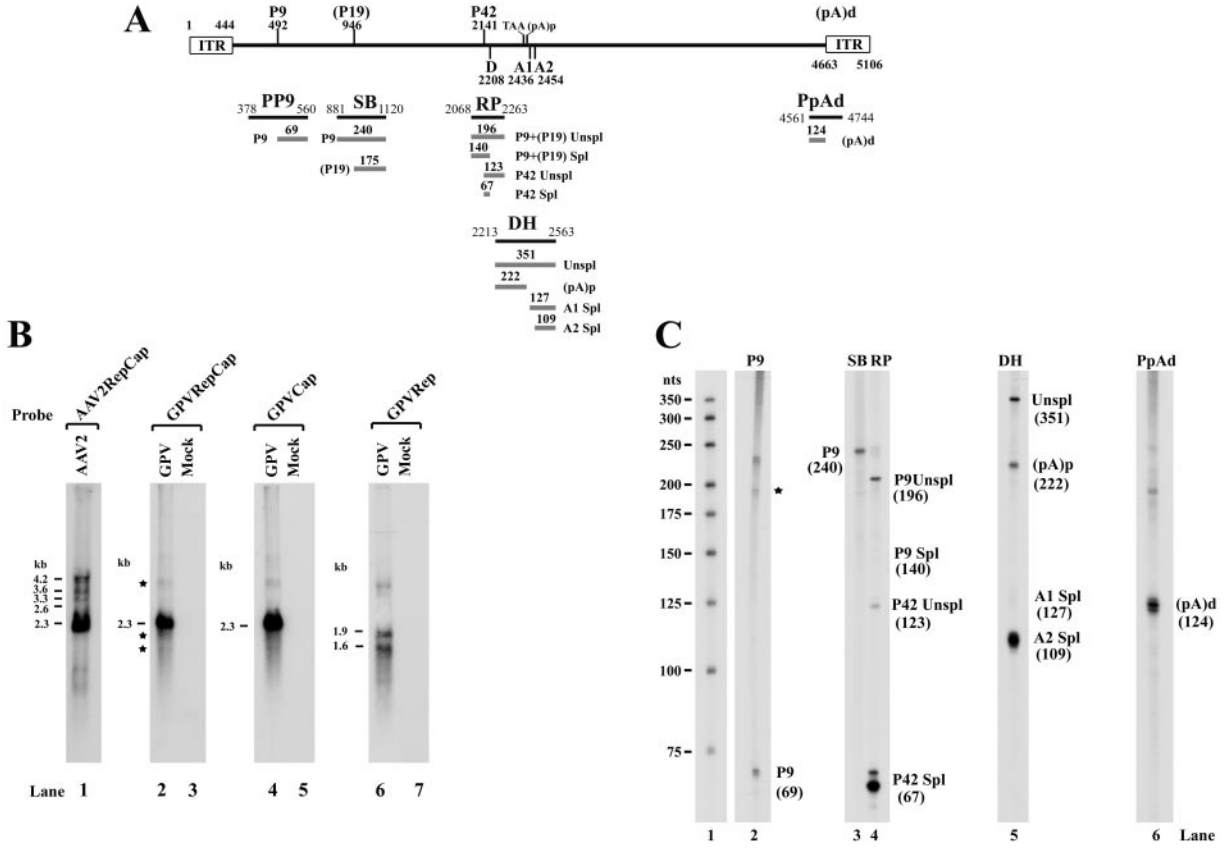

FIG. 1. Initial mapping of GPV transcripts. (A) Diagrammatic representation of the GPV genome. The map shows the nucleotide locations of various landmarks of the GPV genome, established previously or in panels B and C. The putative promoters (P9, P19, and P42), the central intron donor (D) and acceptors (A1 and A2), and the proximal [(pA)p] and distal [(pA)d] polyadenylation sites are shown. The putative P19 promoter is placed in parentheses to indicate that we could not detect its presence by either RNase protection assay (panel C) or by 5′ RACE (Fig. 2B) or Northern analysis (Fig. 2D). The location of the probes used for RNase protection assays shown in panel C are also indicated. PP9 (nt 378 to nt 560), SB (nt 881 to 1120), RP (nt 2608 to 2263), DH (nt 2213 to 2563), PpAd (nt 4561 to 4744), and the bands they were expected to protect are depicted. (B) Northern blot analysis was performed on RNA isolated from CGBQ cells 36 to 40 h posttransfection either with the full-length GPV clone (lanes 2, 4, and 6) or mock transfected (lanes 3, 5, and 7) or, as a size control, from 293 cells infected with AAV2 and adenovirus (lane 1). Northern blots were hybridized with DNA fragments representing either essentially the whole GPV genome (GPVRepCap, nt 314 to 4744) (lanes 2 and 3), a fragment spanning the GPV *cap* gene (GPVCap, nt 3002 to 4744) (lanes 4 and 5), or a fragment spanning the GPV *rep* gene (GPVRep, nt 314 to 1798) (lanes 6 and 7). In addition to the predominant 2.3-kb band, the GPVRepCap probe also detected three minor species, designated by an asterisk in lane 2 and described in the text. The exposure time for lanes 6 and 7 was approximately 10 times longer than for lanes 1 to 5. AAV2 RNA was detected using an AAV2 fragment spanning essentially the whole genome (AAV2RepCap) (lane 1). The sizes of the GPV RNA species are shown. The sizes of the AAV2 transcripts, shown in lane 1, were previously determined (12, 24). (C) RNase protection analysis of GPV RNA generated following transfection of CGBQ cells. Ten micrograms of total RNA isolated 36 to 40 h following transfection of CGBQ cells by pIGPV was protected by the PP9, SB, RP, DH, and P(pA)d probes, as indicated. Lane 1, ^{32}P-labeled RNA ladder (28), with the respective sizes indicated to the left. The origins of the protected bands in lanes 2 to 6 are indicated. Spl, spliced RNA; Unspl, unspliced RNA; (pA)p, RNA polyadenylated at the proximal site; (pA)d, RNA polyadenylated at the distal site. The band designated by a star in lane 2 is most likely due to protection by either a read-around transcript from the plasmid or an RNA generated from the ITR, as previously seen for AAV5 (24).

initiation site for P9-generated RNA at nt 492, 23 nt downstream of the TATA box. The band at approximately 190 nt is likely to result from transcription from the ITR, as has been previously described for AAV5 (24).

The RP probe, which spans the putative P42 promoter and the donor site, protected bands of approximately 196, 123, and 67 nt (Fig. 1C, lane 4). These bands mapped the initiation site of the P42 promoter to nt 2141 and the single central intron donor site to nt 2208. Analogous to the situation in AAV5, GPV RNAs generated from the P42 promoter were spliced to steady-state levels of greater than 90% (Fig. 1C, lane 4, compare the 67-nt "spliced" band to the 123-nt "unspliced" band), while RNAs generated from the P9 promoter were spliced at very low frequency (Fig. 1C, lane 4, compare the putative 140-nt "spliced" band to the 196-nt "unspliced" band).

The DH probe, which spans the putative acceptor sites (A1 and A2) and the putative internal polyadenylation site signal (AAUAAA) at nt 2416, protected bands of approximately 351, 222, 127, and 109 nt (Fig. 1C, lane 5). These bands mapped the central intron acceptors A1 to nt 2436 and A2 to nt 2454 (bands at 127 nt and 109 nt, respectively) and confirmed the utilization of the proximal polyadenylation site (pA)p at nt 2434 (band at 222 nt). Comparison of the RP probe-protected 123-nt band, which reflects both unspliced and (pA)p-polyadenylated P42-generated transcripts, with the 67-nt spliced P42 band (Fig. 1C, lane 4) suggests that the majority of P42-gen-

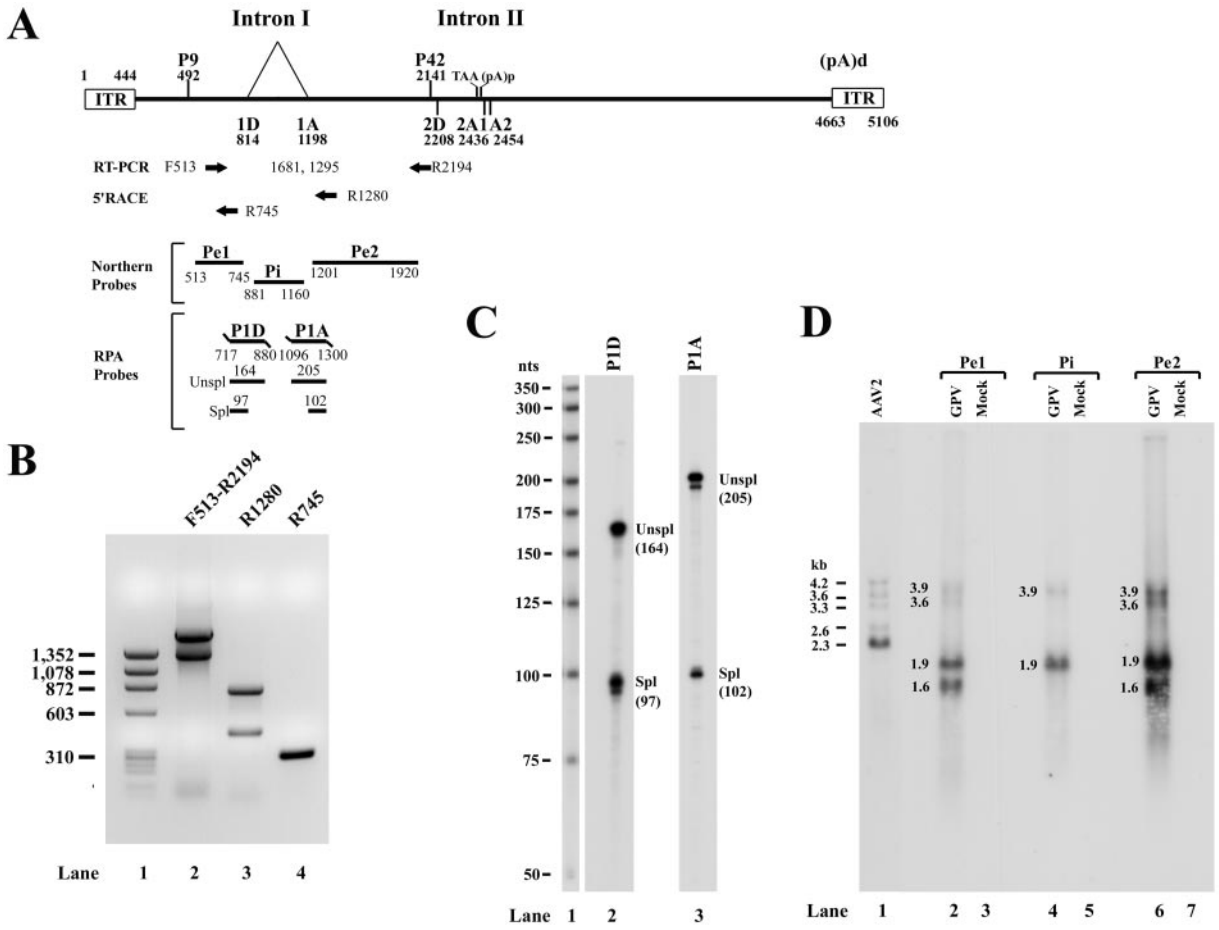

FIG. 2. Identification of an intron within RNA encoded by the *rep* gene of GPV. (A) Probes and primers used for the experiments in panels B to D are schematically diagramed in relation to the GPV genome. The promoters (P9 and P42), the intron donors (1D and 2D) and acceptors (1A, 2A1, and 2A2), and the proximal [(pA)p] and distal [(pA)d] polyadenylation sites are shown and are as in Fig. 1. The locations of RNase protection probes used for the experiment in panel C, P1D (nt 717 to 880) and P1A (nt 1096 to 1300), and the locations of probes for the Northern analysis in panel D, Pe1 (nt 513 to 745), Pi (nt 881 to 1160), and Pe2 (nt 1201 to 1920), are shown. Primers for RT-PCR, F513 and R2194, are shown with the sizes of expected amplified DNA. (B) 5′ RACE and RT-PCR using RNA from GPV-infected CGBQ cells. GPV RNAs were isolated from CGBQ cells 5 to 6 days postinfection with GPV. RT-PCR was performed using the primer set F513 and R2194 (lane 2). 5′ RACE was performed using two reverse primers: R1280 (lane 3) and R745 (lane 4), along with d(T)19V, as described in the text. Lane 1 shows μX174 DNA digested with HaeIII as a size marker. (C) RNase protection analysis across the putative upstream intron donor and acceptor. Ten micrograms of total RNA isolated 36 to 40 h after transfection of CGBQ cells with pIGPV was protected by the P1D (lane 2) and P1A (lane 3) probes as indicated. Lane 1, ^{32}P-labeled RNA ladder, with the respective sizes indicated to the left. The origins of the protected bands in lanes 2 and 3 are indicated. Spl, spliced species; Unspl, unspliced species. (D) Northern blot analysis was performed on RNA isolated 36 to 40 h posttransfection of CGBQ cells using probe Pe1 (lanes 2 and 3), which specifically hybridized to RNA species containing the first exon, probe Pi (lanes 4 and 5), which specifically hybridized to RNA within the putative first intron, and probe Pe2 (lane 6 and 7), which specifically hybridized to RNA species containing the second exon. The sizes of the GPV RNA species are shown. The sizes of AAV2 transcripts used as size markers were previously determined (12, 24) and are shown in lane 1.

erated RNAs read through the (pA)p site and were polyadenylated at the right-hand (pA)d site and ultimately spliced.

The distal polyadenylation site was mapped using the PpAd probe. This probe protected a predominant band of approximately 124 nt (Fig. 1C, lane 6), thus mapping the distal polyadenylation site [(pA)d] to nt 4684.

Northern analysis as described above, using a Rep-specific probe, revealed that two RNA species were generated from the Rep gene region (Fig. 1B, lane 6). The great majority of these RNAs are polyadenylated at the (pA)p site, and an unspliced version of the smaller of the two transcripts would be expected to initiate in the vicinity of nt 930 to 950, which would correspond to initiation from a P19 promoter seen for all AAV serotypes so far examined (19). However, there is neither a consensus TATA nor initiator sequence in the putative P19 region, and the SB probe, which spans the putative P19 promoter region (30), protected only a single band of approximately 240 nt (Fig. 1C, lane 3), suggesting that there is no active promoter in this region. 5′ RACE, using a primer at nt 1280, also generated two bands (Fig. 2B, lane 3); however, DNA sequencing of these products demonstrated that they both initiated at nt 492, 23 nt downstream of the P9 TATA box (data not shown), as did the 5′ RACE product of the primer at nt 745 (Fig. 2B, lane 4; sequence data not shown).

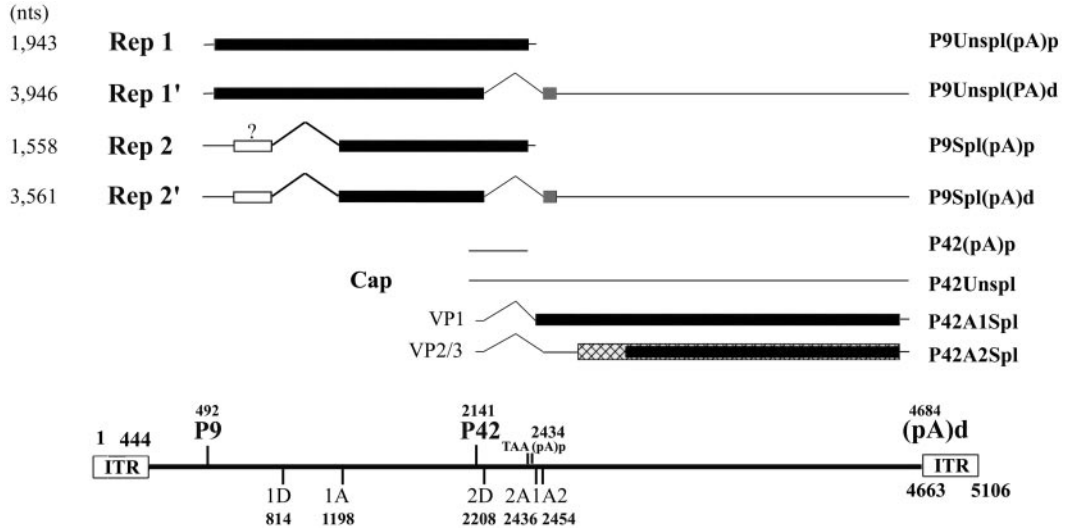

FIG. 3. Transcription map of GPV. The genome of GPV is shown to scale with the major transcription landmarks, including the ITRs, promoters (P), splice donors (D) and acceptors (A), and the proximal [(pA)p] and distal [(pA)d] polyadenylation sites. All species of RNA are shown with designations to the right. The existence of the smaller Rep2 and the open reading frames from which it might be encoded have not yet been established, and this is indicated by the question mark. The different ORFs are shown in boxes with different fill patterns. For clarity of presentation in the Discussion, the ORF indicated by the black box has been arbitrarily designated as ORF 1, the open box has been designated as ORF 2, and the stippled box has been designated as ORF 3. The VP3 protein is presumably encoded in the same frame as VP1 and VP2, from an alternative AUG, as is the case for the AAV capsid proteins, although this has not been demonstrated.

Approximately half of the P9-generated pre-mRNAs are spliced within the Rep1 region. Members of the *Parvovirus* genus use an alternative splicing strategy to generate transcripts encoding additional nonstructural proteins. RT-PCR, using a forward primer (F513) which matches the 5′ end of Rep mRNA, and a reverse primer (R2194) immediately upstream of the central intron donor site (nt 2208), generated two bands of approximately 1,681 and 1,295 nt (Fig. 2B, lane 2). Sequencing of the smaller 1,295-nt band showed that it was spliced between consensus donor and acceptor splice sites at nt 814 to 1198 (data not shown), suggesting that P9-generated pre-mRNAs contain an additional 385-nt intron within the Rep coding region.

RNase protection assays using probes spanning either the putative donor site at nt 814 (probe P1D) (Fig. 2C, lane 2) or the putative acceptor site at nt 1198 (probe P1A) (Fig. 2C, lane 3) confirmed splicing at these sites and demonstrated that the relative steady-state accumulated ratio of spliced and unspliced RNAs was approximately 1:1.

The presence of this spliced transcript was also demonstrated by Northern blot analysis. Probes predicted to hybridize both upstream (probe Pe1, nt 513 to 745) and downstream (probe Pe2, nt 1201 to 1920) of the putative intron detected abundant RNA bands at approximately 1.9 and 1.6 kb (Fig. 2D, lane 2 and 6), while a probe lying wholly within the putative intron (probe Pi, nt 881 to 1160) primarily detected the 1.9-kb RNA species (Fig. 2D, lane 4). These results support the notion that the 1.9- and 1.6-kb bands are P9-generated RNAs which are polyadenylated at (pA)p and either unspliced or spliced as described above. The minor bands (representing $<10\%$ of the total) detected by Pe1 and Pe2 (the 3.9- and 3.6-kb bands) (Fig. 2D, lanes 2 and 6) and by Pi (3.9 kb) (Fig. 2D, lane 4) likely represent molecules that are spliced at the central intron, polyadenylated at the distal polyadenylation site (pA)d, and either unspliced (3.9 kb) or spliced (3.6 kb) between nt 814 and 1198. A genetic map summarizing the results of the experiments so far described is shown in Fig. 3.

Identification of the DSE and USE that govern polyadenylation at the (pA)p site. Alignments of the (pA)p signals and the 3′ splice sites of the central intron of GPV and AAV5 show striking similarity (Fig. 4A). The (pA)p signal of AAV5 contains a U-rich DSE (Fig. 4) approximately 16 nt downstream of the AAUAAA motif, and this DSE overlaps with the polypyrimidine tract of the AAV5 A2 3′ splice site (23). The GPV (pA)p site is also followed by a U-rich region—slightly larger and spanning both sides of the A2 acceptor site—which presumably plays an essential role for cleavage and polyadenylation at GPV (pA)p.

To identify the DSE essential for polyadenylation at (pA)p, we employed a strategy that was successful in identifying the AAV5 DSE. First, we determined that the GPV intron alone was able to support efficient polyadenylation at (pA)p. Polyadenylation at (pA)p was efficient in a construct in which both the *rep* and *cap* genes were replaced with heterologous prokaryotic DNA (PJInJpAd) (Fig. 4B and C, lane 9). A minimal parent plasmid (P9JCapAA) was next constructed from the GPVRepCap plasmid by replacing the *rep* gene (and the embedded P42 promoter) with heterologous sequences from the bacterial plasmid pBR322 and destroying the A2 splice acceptor by mutation of AG\ to AA\. As was the case in AAV5 (23), mutation of the GPV A2 acceptor prevented all splicing of this intron (data not shown). Greater than 90% of the P9-generated RNAs produced by P9JCapAA were polyadenylated at (pA)p (Fig. 4B and C, lane 1).

The potential U-rich DSE sequences are indicated in Fig. 4B. Mutation of the 6-U motif to A residues reduced poly-

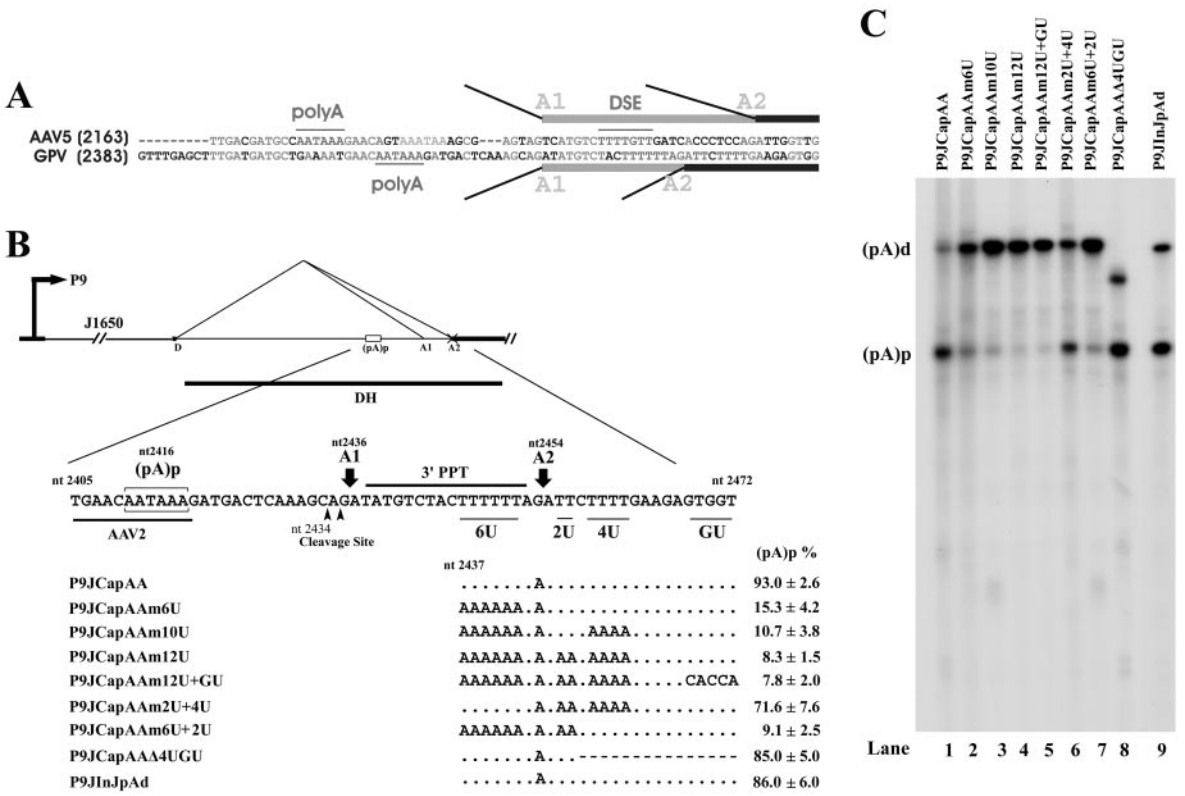

FIG. 4. Characterization of the *cis*-acting DSE that governs GPV polyadenylation at the proximal site [(pA)p]. (A) Alignment of the (pA)p site and central intron acceptor regions of AAV5 and GPV is shown. (B and C) CGBQ cells were transfected with either plasmid P9JCapAA [the (pA)p region is diagrammed], P9JCapAA-based plasmids, which contain various mutations of the putative DSEs, or the P9JInJpAd plasmid (described in the text) (B). Total RNA from CGBQ cells transfected with the plasmids, indicated above each lane, were protected with their homologous DH probes (B). (C) Representative experiment, with the identities of the protected bands shown on the left. Quantification of the ratios of RNAs polyadenylated at (pA)p relative to the total protected RNAs are shown in panel B as averages with standard deviations and are results of at least three individual experiments. RNA from untransfected cells generated no protection products in these experiments (data not shown). The cleavage site diagrammed in panel B was confirmed by 3′ RACE (data not shown). The GPV sequences underlined in panel B are identical to AAV2 sequences in the analogous region of that virus.

adenylation at (pA)p from 93% to 15% (P9JCapAAm6U) (Fig. 4B and C, lane 2). Additional mutation of the 2-U motif reduced polyadenylation at (pA)p to approxi mately 9% (P9JCapAAm6U2U) (Fig. 4B and C, lane 7). Additional mutations made in the 6-U background had little effect (P9JCapAAm10U, P9JCapAAm12U, and P9JCapAAm12U+GU) (Fig. 4B and C, lanes 3 to 5), and mutations of the 2U+4U motifs alone, or deletion of 4U region, had little effect (P9JCapAAm2U+4U [Fig. 4, lane 6] and P9JCapAAΔ4UGU [Fig. 4B and C, lane 8]). These results suggested that the 6-U motif that lies within the GPV A2 3′ splice site comprised the core DSE, governing the majority of the polyadenylation at (pA)p, and the 2-U and 4-U motifs that lie after the A2 3′ splice site likely also participate. When placed in a splicing-competent background, the 6-U mutation significantly decreased splicing of the central intron (data not shown), suggesting that, similar to AAV5, overlapping signals required for these two processes likely lead to a competition between these processes.

For their efficient use, some polyadenylation signals also require a region upstream of the AAUAAA motif. Such USEs are often GU rich. Mutation of the region upstream of the GPV (pA)p site in the splicing-deficient parent plasmid P9JCapAA identified an element essential for its efficient usage. Replacement of nt 2219 to nt 2390 with heterologous prokaryotic plasmid DNA reduced polyadenylation at (pA)p from 93% to 8.5% (Fig. 5A and B, lanes 1 and 6; compare P9JCapAA and P9JIm170CapAA). A similar reduction in polyadenylation at (pA)p was seen following substitution of a smaller region from either nt 2262 or nt 2304 to nt 2390 (P9JIm120CapAA and P9JIm80CapAA) (Fig. 5A and B, lanes 2 and 3). Substitution of the region between nt 2346 and 2390 (P9Jm40CapAA) (Fig. 5A and B, lane 4) allowed a slightly greater level of polyadenylation at (pA)p; however, the efficiency was still reduced from 93% to 16%. Substitution with ACACAAA in place of the GU-rich motif (TGTGTTT) within this region resulted in only a partial reduction in polyadenylation (P9JmGUCapAA) (Fig. 5A and B, lane 5). Thus, the region upstream of the (pA)p site represents an authentic USE; however, the exact sequences responsible for this effect remain to be completely defined.

The Rep protein of GPV potently transactivates the P42 promoter via binding upstream of the TATA box. As shown by both Northern and RNase protection analyses described above, P42-generated RNAs comprised approximately 90% of the RNA generated by GPV in CGBQ cells following trans-

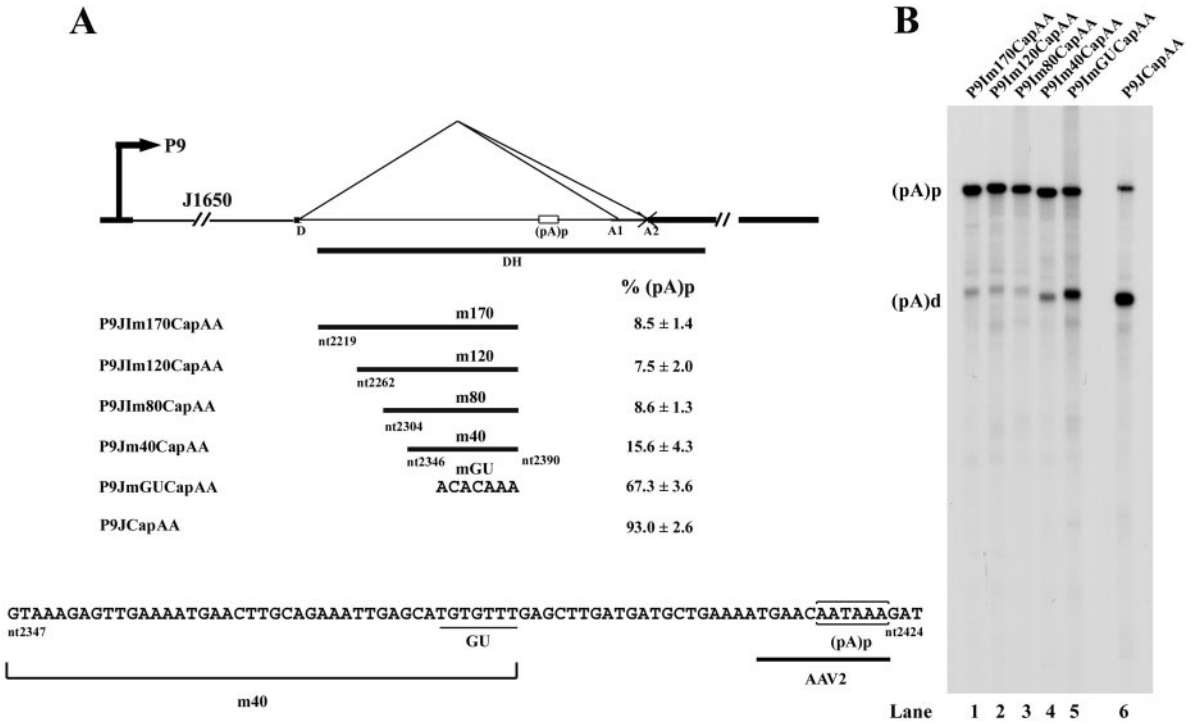

FIG. 5. Characterization of the *cis*-acting USE that governs GPV polyadenylation at the proximal site [(pA)p]. (A) P9JCapAA-based plasmids which contain various mutations of the putative USE are diagrammed, and the locations of the mutations relative to the (pA)p site are shown. (B) Total RNAs taken from CGBQ cells transfected with these plasmids, as indicated above each lane, were protected with their homologous DH probes. A representative experiment is shown, with the identities of the protected bands shown on the left. Quantifications of the ratios of RNAs polyadenylated at (pA)p relative to the total protected RNAs are shown in panel A as averages with standard deviations and are results of at least three individual experiments. Sequences underlined in panel A are identical to AAV2 sequences in the analogous region of that virus.

fection of either the ITR-containing infectious clone (Fig. 1C, lane 4), or the RepCap construct with the ITR deleted (Fig. 6A, lane 1). Expression of P42 was dependent on the Rep1 protein, because a translation termination signal inserted early into the Rep coding region of RepCap (at nt 612) abolished expression from P42 (Fig. 6A, lane 3) and expression of P42 from this construct could be rescued by adding Rep1 in *trans* (Fig. 6, lane 4). Expression of P9 was independent of Rep1 (Fig. 6A, lanes 3 and 4).

GPV Rep1 shares a high degree of homology to the AAV2 Rep 78, although they do not complement for replication (29). For AAV2, a Rep binding site either in P5 or the AAV2 ITR is required for transactivation of the AAV2 P40 promoter by AAV2 Rep (17, 18, 21). The GPV P9 TATA box is only 16 nt downstream of the terminus of the left-hand ITR, and there is a single GPV RBE upstream (GTTCGAACGAACGAAC, nt 380 to 395 [28]). As expected, deletion of nt 314 to 446 from the RepCap plasmid, which removes the P9 promoter and RBE, prevented detectable constitutive expression from the plasmid but, surprisingly, did not prevent activation of P42 when Rep1 was supplied in *trans* (GPVΔP9RepCap) (Fig. 6A, lanes 5 and 6).

There are two degenerate RBEs just upstream of the P42 promoter (Fig. 6B), and it seemed possible, as is the case for the autonomous parvovirus MVM (2), that a binding site immediately upstream of the TATA box could mediate Rep1 transactivation of P42. Indeed, in a minimal construct in which only 56 nt upstream of the P42 TATA sequence containing these sites was retained, the P42 promoter remained fully activatable by Rep1 supplied in *trans* (GPVP42Cap) (Fig. 6A, lanes 7 and 8).

A map of the sequence upstream of P42, showing the positions of the two putative degenerate Rep1 binding sites, is presented in Fig. 6B. When either the upstream RBE1 alone was deleted (2034P42Cap) (Fig. 6B, lanes 3 and 4) or either of the two sites was individually mutated (P42mRBE1Cap or P42mRBE2Cap) (Fig. 6B, lanes 5 to 8), the P42 minimal plasmid remained transactivatable by Rep1 supplied in *trans*. However, when the two putative RBEs were either both deleted or destroyed by mutation, activation by Rep1 of P42 was either lost (2056P42Cap) (Fig. 6B, lanes 1 and 2) or reduced by greater than 90% (P42mRBECap) (Fig. 6B, lanes 9 and 10). These results suggested that a single Rep1 binding site was both necessary and sufficient to allow transactivation by GPV Rep1. Adding back two copies of a synthetic consensus Rep1 RBE restored full activity to P42mRBECap (2×RBEP42mRBECap) (Fig. 6B, lanes 12 and 11). Therefore, in contrast to AAV2 but similar to MVM and other members of the *Parvovirus* genus, GPV Rep1 could transactivate its capsid gene via binding to a site on the genome immediately upstream of the promoter.

DISCUSSION

Although GPV has identical hairpin termini, is most similar in both nucleotide sequence and protein homology to AAV2

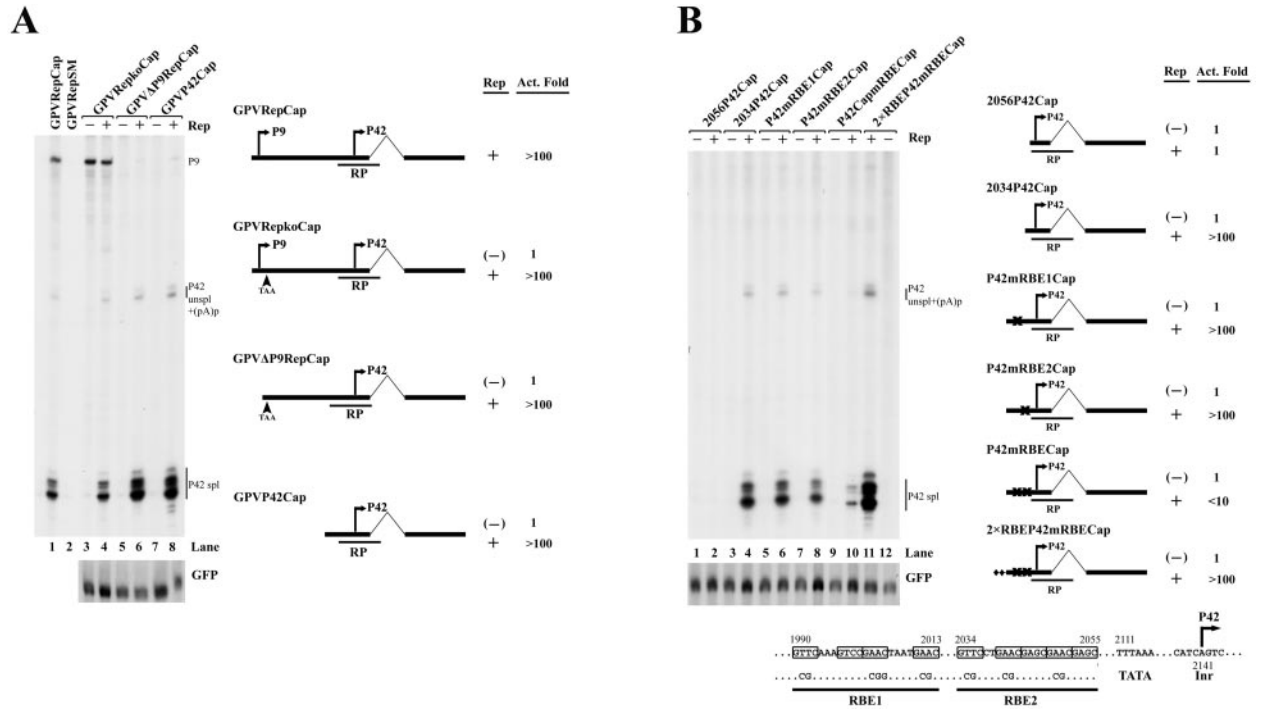

FIG. 6. Rep1 transactivates the P42 promoter in a DNA binding-dependent manner. (A) Plasmids (GPVRepCap, GPVRepkoCap, GPVΔP9RepCap, and GPVP42Cap), which are diagrammed to the right and described in the text, were transfected into CGBQ cells either with or without cotransfection of the Rep-supplementing plasmid GPVRepSM (Rep + and −, respectively). Plasmid pGFPC1 was included as an internal control. Total RNA, isolated 36 to 40 h posttransfection, was protected by the RP probe, shown under the plasmid diagrams. The bands protected specifically by either P9-generated RNA or by spliced or unspliced P42-generated RNA from a representative experiment are shown. As described in the Materials and Methods section, the RP probe was designed to specifically hybridize to RNAs generated from the reporter plasmids and not the Rep-supplementing plasmid GPVRepSM (lane 2). Quantifications of the abundance of P42-generated spliced (sp) and unspliced (unspl) RNAs are shown following standardization relative to bands protected by the cotransfected standard GFP RNA. At least three separate experiments were performed. (B) A detailed diagram of the P42 promoter is shown on the bottom. The putative Inr sequence, TATA box, and the potential RBEs are shown. Mutations of RBE-like sequences are indicated under the P42 sequences. Plasmids diagrammed to the right and described in the text were transfected into CGBQ cells either with [Rep (+)] or without [Rep (−)] cotransfection of the Rep-supplementing plasmid GPVRepSM. GFP-expressing plasmid pGFPC1 was included as an internal control. Total RNAs were protected by the RP probe, whose location is shown. Bands protected specifically by P42-generated RNAs from a representative experiment are shown. Quantifications of the abundance of P42-generated RNAs, including both unspliced (unspl), proximally polyadenylated [(pA)p], and spliced (spl) RNA, were determined by dividing the signals due to P42 RNA in the presence of Rep by that in Rep's absence, after standardizing to the cotransfected standard GFP signal. At least three separate experiments were performed.

(30), and has been classified as a member of the *Dependovirus* genus (6), GPV can replicate efficiently without the aid of helper virus (9). We have determined the RNA expression profile of GPV and find that it is a surprising hybrid of features of the *Parvovirus* and *Dependovirus* genera of the *Parvovirinae* subfamily of the *Parvoviridae*. Similar to the *Dependovirus* AAV5, RNAs transcribed from the GPV P9 promoter (P7 for AAV5), which for GPV encodes the viral Rep1 protein and presumably a smaller Rep protein as well, were polyadenylated at a high efficiency at the polyadenylation site (pA)p located within the small intron in the center of the genome. Surprisingly, no promoter analogous to the *Dependovirus* P19 promoter was detected; however, similar to MVM and other members of the *Parvovirus* genus (19), a significant portion of pre-mRNAs generated from the P9 promoter were additionally spliced within the putative GPV Rep1 coding region, between a donor site located at nucleotide 814 and an acceptor site at nucleotide 1198. Additionally, we found that similar to the *Parvovirus* MVM (5, 8, 11), detectable activity of the GPV P42 promoter was highly dependent on transactivation by the GPV Rep1 protein in a manner dependent on Rep1 binding to a *cis*-element located just upstream of the P42 promoter.

The generation of multiple nonstructural proteins is achieved in different ways by different parvoviruses. All members of the *Dependovirus* genus so far examined utilize a promoter in the Rep gene region (the P19 promoter for AAV2 and AAV5) to produce a set of smaller RNAs that generate a set of smaller Rep proteins (19). MVM and other members of the *Parvovirus* genus use alternative splicing of the NS gene pre-mRNAs to generate mRNAs that encode such proteins. In all cases these expression strategies ensure that the smaller nonstructural proteins contain at least a partial subset of amino acids also contained within the larger proteins (19). Although not fully characterized, the smaller nonstructural proteins of both genera perform functions that are at least somewhat related, suggesting that these two genera have evolved separate mechanisms to accommodate a similar requirement for replication. Although a member of the *Dependovirus* genus, the mechanism that GPV uses for this purpose is more like that used by members of the *Parvovirus* group. Comparison of the

available sequences of the GPV and MDPV *rep* genes showed that the donor and acceptor sites of the intron within the *rep* gene are highly conserved (data not shown).

There are two potential coding strategies for a smaller Rep protein from spliced RNA. If the putative smaller Rep protein used the same initiating AUG at nt 536 as Rep1 (ORF 1), these proteins would share N-terminal amino acid sequence until the splice site at nt 814, and then, in the spliced RNA, the smaller Rep would continue in ORF 3 until reaching a termination codon at nt 1249. This strategy, in which N-terminal sequence is shared and which would generate a protein of 109 amino acids, would be similar to the coding strategy for NS1 and NS2 of MVM. Alternatively, the putative smaller Rep protein could be initiated in ORF 2 at an AUG at nt 650. The 55 N-terminal amino acids of the two proteins would thus be different; however, splicing between nt 814 and 1198 would return the smaller protein reading frame back to that of Rep1 ORF 1. This smaller Rep protein would be 460 amino acids in length and, using this strategy, the GPV proteins would share C-terminal sequences, similar to the AAV2 Rep78 and Rep52 proteins. The strategy by which the GPV *rep* gene RNAs encode the corresponding nonstructural proteins is currently under investigation.

Like AAV5 (24), GPV uses a polyadenylation signal in the center of its genome. Greater than 90% of the P9-generated RNAs polyadenylate at (pA)p. As mentioned above, in contrast to AAV5, approximately half of the P9-generated transcripts that are polyadenylated at (pA)p are also spliced upstream in the *rep* gene region. A similar polyadenylation signal is also present in the A1 acceptor site of the central intron of MDPV, and efficient polyadenylation at that site has also been observed (Qiu and Pintel, unpublished). Interestingly, a similar AAUAAA motif is also found within the central intron of the closely related AAV2; however, polyadenylation at this site is not detectable by RPA (Qiu and Pintel, unpublished). Efficient polyadenylation at the GPV (pA)p requires auxiliary signals (DSE and USE), and such signals are likely critical for controlling internal polyadenylation in parvoviral RNA processing. Sequence comparison of a number of GPV isolates demonstrates a conserved DSE signal in the A2 3′ acceptor region (Vilmos Palya, personal communication). For both AAV5 and GPV, these signals overlap with signals that govern cleavage of the 3′ splice site of the central intron, and competition between splicing and polyadenylation influences expression of these genomes. Further characterization of the DSEs and USEs that modulate (pA)p also may provide an avenue to determine why the identical poly(A) signal in AAV2 is not used and why AAV2 has evolved so as to make internal polyadenylation nonessential.

For both the *Parvovirus* and *Dependovirus* genera, full activity of the capsid gene promoter requires transactivation by the viral Rep protein (17, 18, 21). This mechanism presumably restricts expression of capsids until a time in the viral life cycle when they are necessary. The one characterized exception is AAV5, whose capsid gene expression is constitutively high in 293 cells (24). For AAV2, transactivation of the P40 promoter by Rep is accomplished via binding to RBEs either in the upstream ITR or the upstream P5 promoter (17, 18, 21). For MVM, transactivation of the P38 promoter can be achieved following binding to NS1 binding sites in the transactivation response region upstream of P38 (2). For MVM, there are multiple NS1 binding sites throughout the genome (3), and they have been shown to be at least somewhat redundant in their ability to mediate NS1 activation of MVM P38 (15). In contrast, other than a site within the ITR, the only other RBE-like motifs in the GPV genome are those described in Fig. 6B, upstream of P42. Although Rep1 of GPV has substantial similarity to the AAV2 Rep78 protein, its mode of activation is more similar to the NS-1 protein of MVM. Perhaps the fact that the GPV Rep1 can so potently activate the GPV capsid gene promoter in this manner contributes to its independence from helper virus.

The activation domain of MVM NS1 has been localized to the 126 C-terminal amino acids of NS-1 (13). Interestingly, the C terminal (147 amino acids) of GPV Rep1 is the region most distinct for the analogous region in AAV2 Rep78, with only 22% identity (28). This region of GPV Rep1 lies within the central intron and would be removed upon splicing of the intron. Perhaps polyadenylation at (pA)p ensures that these RNAs are not spliced and that this region of GPV Rep1 can be expressed.

The expression profile of the autonomously replicating *Dependovirus* GPV exhibits features that have been shown previously to be present exclusively in either the *Parvovirus* or *Dependovirus* genus. It thus seems possible that GPV may represent an evolutionary variant, intermediate, or precursor and that its further study may provide insight into parvovirus evolution.

ACKNOWLEDGMENTS

We thank Lisa Burger for excellent technical assistance and Gregory E. Tullis for critical reading of the manuscript. We are grateful to Kevin Brown (National Institutes of Health) for providing cells and clones of GPV, which helped initiate this study, and to Michael Linden for plasmids, advice, and discussion. We also thank Vilmos Palya at CEVA-Phylaxia Veterinary Biologicals Co. Ltd., Hungary, for sharing unpublished information.

This work was supported by PHS grants RO1 AI46458 and RO1 AI56310 from NIAID to D.P.

REFERENCES

1. **Brown, K. E., S. W. Green, and N. S. Young.** 1995. Goose parvovirus–an autonomous member of the dependovirus genus? Virology **210:**283–291.
2. **Christensen, J., S. F. Cotmore, and P. Tattersall.** 1995. Minute virus of mice transcriptional activator protein NS1 binds directly to the transactivation region of the viral P38 promoter in a strictly ATP-dependent manner. J. Virol. **69:**5422–5430.
3. **Cotmore, S. F., J. Christensen, J. P. Nuesch, and P. Tattersall.** 1995. The NS1 polypeptide of the murine parvovirus minute virus of mice binds to DNA sequences containing the motif [ACCA]2–3. J. Virol. **69:**1652–1660.
4. **Derzsy, D.** 1967. A viral disease of goslings. I. Epidemiological, clinical, pathological and aetiological studies. Acta Vet. Acad. Sci. Hung. **17:**443–448.
5. **Doerig, C., B. Hirt, P. Beard, and J. P. Antonietti.** 1988. Minute virus of mice non-structural protein NS-1 is necessary and sufficient for trans-activation of the viral P39 promoter. J. Gen. Virol. **69:**2563–2573.
6. **Fauquet, C. M., M. A. Mayo, J. Maniloff, U. Desselberger, and L. A. Ball.** 2004. Virus taxonomy, VIIIth report of the ICTV. Elsevier/Academic Press, London, England.
7. **Francki, R. I. B., C. M. Fauquet, D. L. Knudson, and F. Brown.** 1991. Classification and nomemclature of viruses: fifth report of the International Committee on Taxonomy of Viruses. Springer-Verlag, New York, N.Y.
8. **Gavin, B. J., and D. C. Ward.** 1990. Positive and negative regulation of the minute virus of mice P38 promoter. J. Virol. **64:**2057–2063.
9. **Kisary, J.** 1979. Interaction in replication between goose parvovirus strain B and duck plague herpesvirus. Arch. Virol. **59:**81–88.
10. **Kisary, J., and D. Derzsy.** 1974. Viral disease of goslings. IV. Characterization of the causal agent in tissue culture system. Acta Vet. Acad. Sci. Hung. **24:**287–292.
11. **Krauskopf, A., O. Resnekov, and Y. Aloni.** 1990. A *cis* downstream element

participates in regulation of in vitro transcription initiation from the P38 promoter of minute virus of mice. J. Virol. **64:**354–360.
12. **Laughlin, C. A., H. Westphal, and B. J. Carter.** 1979. Spliced adenovirus-associated virus RNA. Proc. Natl. Acad. Sci. USA **76:**5567–5571.
13. **Legendre, D., and J. Rommelaere.** 1994. Targeting of promoters for *trans* activation by a carboxy-terminal domain of the NS-1 protein of the parvovirus minute virus of mice. J. Virol. **68:**7974–7985.
14. **Liu, Z., J. Qiu, F. Cheng, Y. Chu, Y. Yoto, M. G. O'Sullivan, K. E. Brown, and D. J. Pintel.** 2004. Comparison of the transcription profile of simian parvovirus with that of the human erythrovirus B19 reveals a number of unique features. J. Virol. **78:**12929–12939.
15. **Lorson, C., L. R. Burger, M. Mouw, and D. J. Pintel.** 1996. Efficient transactivation of the minute virus of mice P38 promoter requires upstream binding of NS1. J. Virol. **70:**834–842.
16. **Malkinson, M., and E. Winocour.** 2005. Adeno-associated virus type 2 enhances goose parvovirus replication in embryonated goose eggs. Virology **336:**265–273.
17. **McCarty, D. M., D. J. Pereira, I. Zolotukhin, X. Zhou, J. H. Ryan, and N. Muzyczka.** 1994. Identification of linear DNA sequences that specifically bind the adeno-associated virus Rep protein. J. Virol. **68:**4988–4997.
18. **McCarty, D. M., J. H. Ryan, S. Zolotukhin, X. Zhou, and N. Muzyczka.** 1994. Interaction of the adeno-associated virus Rep protein with a sequence within the A palindrome of the viral terminal repeat. J. Virol. **68:**4998–5006.
19. **Muzyczka, N., and K. I. Berns.** 2001. Parvoviridae: the viruses and their replication, p. 2327–2359. *In* B. N. Fields, P. M. Howley, D. E. Griffin, R. A. Lamb, M. A. Martin, B. Roizman, S. E. Straus, and D. M. Knipe (ed.), Fields virology, 4th ed. Lippincott-Raven Publishers, Philadelphia, Pa.
20. **Naeger, L. K., R. V. Schoborg, Q. Zhao, G. E. Tullis, and D. J. Pintel.** 1992. Nonsense mutations inhibit splicing of MVM RNA in cis when they interrupt the reading frame of either exon of the final spliced product. Genes Dev. **6:**1107–1119.
21. **Pereira, D. J., D. M. McCarty, and N. Muzyczka.** 1997. The adeno-associated virus (AAV) Rep protein acts as both a repressor and an activator to regulate AAV transcription during a productive infection. J. Virol. **71:**1079–1088.
22. **Pintel, D., D. Dadachanji, C. R. Astell, and D. C. Ward.** 1983. The genome of minute virus of mice, an autonomous parvovirus, encodes two overlapping transcription units. Nucleic Acids Res. **11:**1019–1038.
23. **Qiu, J., R. Nayak, and D. J. Pintel.** 2004. Alternative polyadenylation of adeno-associated virus type 5 RNA within an internal intron is governed by both a downstream element within the intron 3′ splice acceptor and an element upstream of the P41 initiation site. J. Virol. **78:**83–93.
24. **Qiu, J., R. Nayak, G. E. Tullis, and D. J. Pintel.** 2002. Characterization of the transcription profile of adeno-associated virus type 5 reveals a number of unique features compared to previously characterized adeno-associated viruses. J. Virol. **76:**12435–12447.
25. **Qiu, J., and D. J. Pintel.** 2002. The adeno-associated virus type 2 Rep protein regulates RNA processing via interaction with the transcription template. Mol. Cell. Biol. **22:**3639–3652.
26. **Schettler, C. H.** 1971. Virus hepatitis of geese. II. Host range of goose hepatitis virus. Avian Dis. **15:**809–823.
27. **Schoborg, R. V., and D. J. Pintel.** 1991. Accumulation of MVM gene products is differentially regulated by transcription initiation, RNA processing and protein stability. Virology **181:**22–34.
28. **Smith, D. H., P. Ward, and R. M. Linden.** 1999. Comparative characterization of Rep proteins from the helper-dependent adeno-associated virus type 2 and the autonomous goose parvovirus. J. Virol. **73:**2930–2937.
29. **Yoon, M., D. H. Smith, P. Ward, F. J. Medrano, A. K. Aggarwal, and R. M. Linden.** 2001. Amino-terminal domain exchange redirects origin-specific interactions of adeno-associated virus Rep78 in vitro. J. Virol. **75:**3230–3239.
30. **Zadori, Z., R. Stefancsik, T. Rauch, and J. Kisary.** 1995. Analysis of the complete nucleotide sequences of goose and muscovy duck parvoviruses indicates common ancestral origin with adeno-associated virus 2. Virology **212:**562–573.